Omicron-induced interferon signalling prevents influenza A virus infection

Running title: Omicron inhibits influenza A virus infection

Denisa Bojkova[1], Marco Bechtel[1], Tamara Rothenburger[1], Joshua D. Kandler[1], Lauren Hayes[2], Ruth Olmer[3], Martin Ulrich[3], Danny Jonigk[4,5], Sandra Ciesek[1,6,7], Mark N. Wass[2], Martin Michaelis[2]*, Jindrich Cinatl jr.[1,8]*

[1] Institute for Medical Virology, University Hospital, Goethe University, Frankfurt am Main, Germany

[2] School of Biosciences, University of Kent, Canterbury CT2 7NJ, UK

[3] Leibniz Research Laboratories for Biotechnology and Artificial Organs (LEBAO), Department of Cardiothoracic, Transplantation and Vascular Surgery (HTTG), REBIRTH-Research Center for Translational Regenerative Medicine, Biomedical Research in Endstage and Obstructive Lung Disease Hannover (BREATH), German Center for Lung Research (DZL), Hannover Medical School, Carl-Neuberg-Straße 1, 30625 Hannover, Germany

[4] Institute of Pathology, Hannover Medical School (MHH), Carl-Neuberg-Straße ,1 30625 Hannover, Germany

[5] Biomedical Research in Endstage and Obstructive Lung Disease Hannover (BREATH), The German Center for Lung Research (Deutsches Zentrum für Lungenforschung, DZL), Hannover Medical School (MHH), Carl-Neuberg-Straße 1, 30625 Hannover, Germany

[6] German Center for Infection Research, DZIF, External partner site, Theodor-Stern-Kai 7, 60590 Frankfurt am Main, Germany

[7] Fraunhofer Institute for Molecular Biology and Applied Ecology (IME), Branch Translational Medicine und Pharmacology, Theodor-Stern-Kai 7, 60590 Frankfurt am Main, Germany

[8] Dr. Petra Joh-Forschungshaus, Komturstr. 3A, 60528 Frankfurt am Main, Germany

* Corresponding authors:

Jindrich Cinatl jr., Institute for Medical Virology, University Hospital, Goethe University, Paul Ehrlich-Straße 40, 60596 Frankfurt am Main, Germany; phone +49 69 6301 6409; e-mail Cinatl@em.uni-frankfurt.de

Martin Michaelis, School of Biosciences, University of Kent, Canterbury CT2 7NJ, UK; phone +44 1227 82 7804; e-mail M.Michaelis@kent.ac.uk

Abstract

Recent findings in permanent cell lines suggested that SARS-CoV-2 Omicron BA.1 induces a stronger interferon response than Delta. Here, we show that BA.1 and BA.5 but not Delta induce an antiviral state in air-liquid interface (ALI) cultures of primary human bronchial epithelial (HBE) cells and primary human monocytes. Both Omicron subvariants caused the production of biologically active type I (α/β) and III (λ) interferons and protected cells from super-infection with influenza A viruses. Notably, abortive Omicron infection of monocytes was sufficient to protect monocytes from influenza A virus infection. Interestingly, while influenza-like illnesses surged during the Delta wave in England, their spread rapidly declined upon the emergence of Omicron. Mechanistically, Omicron-induced interferon signalling was mediated via double-stranded RNA recognition by MDA5, as MDA5 knock-out prevented it. The JAK/ STAT inhibitor baricitinib inhibited the Omicron-mediated antiviral response, suggesting it is caused by MDA5-mediated interferon production, which activates interferon receptors that then trigger JAK/ STAT signalling. In conclusion, our study 1) demonstrates that only Omicron but not Delta induces a substantial interferon response in physiologically relevant models, 2) shows that Omicron infection protects cells from influenza A virus super-infection, and 3) indicates that BA.1 and BA.5 induce comparable antiviral states.

Keywords: SARS-CoV-2; COVID-19; interferon; monocytes; influenza; super-infection; antiviral state; BA.1; BA.5; Delta

Introduction

SARS-CoV-2, the coronavirus that causes COVID-19, has caused the worst pandemic since the Spanish Flu in 1918-1920 [Bastard et al., 2022]. Virus-induced interferon signalling has been shown to be critically involved in determining COVID-19 severity [Bastard et al., 2022; Chiale et al., 2022]. Individuals with defects in their interferon response are predisposed to life-threatening COVID-19 [Bastard et al., 2022; Chiale et al., 2022], and a particularly pronounced interferon-related innate immune response is anticipated to contribute to the lower COVID-19 severity observed in children [Borrelli et al., 2021].

Recent findings suggested that SARS-CoV-2 Omicron BA.1 displays a lower interferon antagonism than Delta [Bojkova et al., 2022; Bojkova et al., 2022a]. BA.1 and Delta viruses showed a similar replication pattern in interferon-deficient Vero cells, but BA.1 replication was attenuated relative to Delta in interferon competent Calu-3, Caco-2, and Caco-2-F03 (a highly SARS-CoV-2-susceptible Caco-2 subline [Bojkova et al., 2022b]) cells [Bojkova et al., 2022; Hu et al., 2022; Shuai et al., 2022]. Moreover, BA.1 induced a more pronounced interferon response than Delta [Bojkova et al., 2022; Bojkova et al., 2022a].

Here, we investigated Delta, BA.1, and BA.5 replication in air-liquid interface (ALI) cultures of primary human bronchial epithelial (HBE) cells and primary human monocytes. To examine whether SARS-CoV-2-induced interferon induction results in a biologically relevant antiviral state, we further determined the impact of Delta, BA.1, and BA.5 infection on influenza A virus replication in ALI HBE cultures (H1N1) and monocytes (H1N1, H5N1), as interferon signalling is considered to be a major influenza A virus restriction factor [McKellar et al., 2021].

Results

Infection kinetics and interferon response induction by Omicron BA.1 and Delta in air-liquid-interface (ALI) cultures of primary human bronchial epithelial (HBE) cells

BA.1 displayed faster replication kinetics than Delta in ALI HBE cultures (Figure 1), as indicated by high SARS-CoV-2 nucleoprotein (NP), genomic RNA levels, and caspase 3/7 activity (which reflects SARS-CoV-2 replication independently of whether the virus causes cytotoxicity resulting in a cytopathogenic effect in a cell culture model [Bojkova et al., 2022b]) (Figure 1B-D). However, the replication of both SARS-CoV-2 variants resulted in comparable peak NP and genomic RNA levels (Figure 1B-D). While the BA.1 levels declined after a peak (at 24h post infection for NP and 72h for genomic RNA), Delta levels continued to increase until 120h post infection (Figure 1B-D). These findings are in accordance with previous findings showing that BA.1 replicates faster than other variants in bronchial cells [Hui et al., 2022]. Independently of the replication kinetics BA.1 and Delta caused similar reductions of the ALI HBE barrier integrity (Figure 1E).

Also in agreement with previous findings [Alfi et al., 2022; Bojkova et al., 2022; Bojkova et al., 2022a], BA.1 induced a stronger interferon response than Delta, as indicated by the abundance and phosphorylation levels of a range of proteins involved in interferon signalling (Figure 1F). Moreover, only BA.1 but not Delta induced the secretion of biologically active interferon-α/β (Figure 1G) and -λ (Figure 1H) by ALI HBE cultures, as demonstrated using HEK-reporter cell lines.

Figure 1

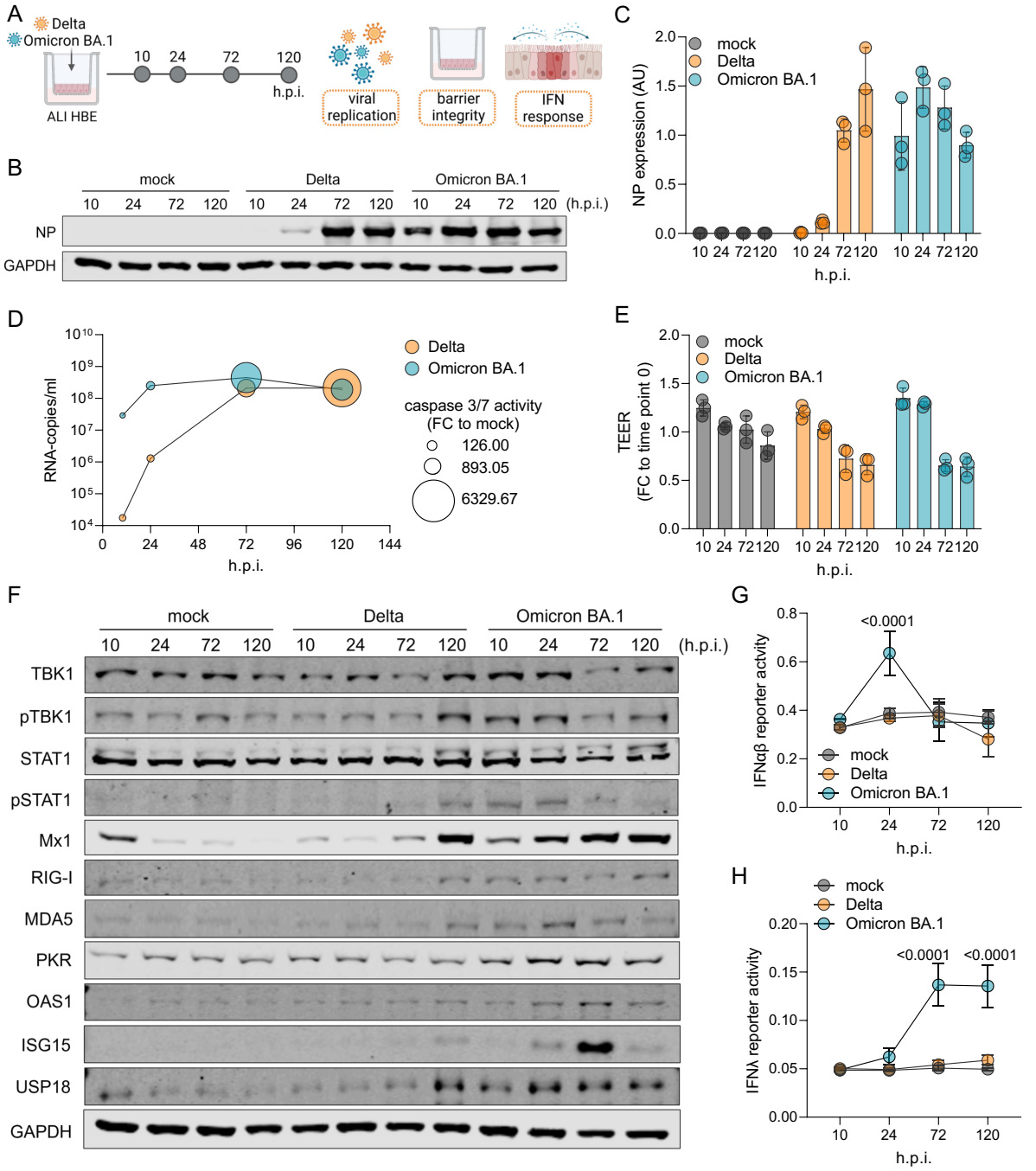

Figure 1. Infection kinetics and interferon response induction by Omicron BA.1 and Delta in air-liquid-interface (ALI) cultures of primary human bronchial epithelial (HBE) cells. (A) Schematic depiction of the experimental set-up. (B) Immunoblot of cellular SARS-CoV-2 nucleoprotein (NP) levels in BA.1- and Delta (MOI 1)-infected ALI HBE cultures at different time points post infection. (C) Quantification of NP levels (mean ± SD) by ImageJ. (D) SARS-CoV-2 genomic RNA copy numbers

(Y axis) and caspase 3/7 activity (bubble size) determined in the apical medium of BA.1- and Delta (MOI 1)-infected at different time points post infection. (E) Evaluation of barrier integrity by measurement of TEER in BA.1- and Delta (MOI 1)-infected ALI HBE cultures at different time points post infection. Bars represents mean ± SD of three biological replicates. (F) Immunoblot indicating cellular levels of proteins involved in interferon signalling in BA.1- and Delta (MOI 1)-infected ALI HBE cultures at different time points post infection. (G,H) Interferon (IFN)-α/β (G) and IFNλ (H) responses induced in HEK reporter cell lines by apical washes from BA.1- and Delta (MOI 1)-infected ALI HBE cultures collected at different time points post infection. P values were determined by one-way ANOVA with subsequent Tukey's test.

Interferon-α/β peaked at 24h post infection (Figure 1G), which was followed by a return to basal levels, whereas interferon-λ remained elevated until 120h post infection (Figure 1H). Short-term interferon type I (α/β) responses cause a protective antiviral response, while long-term interferon activity is associated with potentially deleterious inflammation [Forero et al., 2019; King & Sprent, 2021]. In contrast, sustained interferon type III (λ) responses inhibit respiratory virus replication at epithelial barriers in the respiratory tract and prevent excessive inflammation [Forero et al., 2019; Prokunina-Olsson et al., 2020; King & Sprent, 2021]. Hence, the interferon type I and III responses observed in BA.1-infected ALI HBE cultures add further evidence explaining why Omicron is less pathogenic than other SARS-CoV-2 variants like Delta [Wang et al., 2022].

JAK/ STAT inhibition suppresses BA.1-induced interferon signalling and increases BA.1 replication in air-liquid-interface (ALI) human bronchial epithelial (HBE) cell cultures

Interferon signalling can be induced in a STAT1-dependent and -independent manner [Rani et al., 2010; Bastard et al., 2022; Chiale et al., 2022]. In hibition of JAK/ STAT signalling using the JAK inhibitor baricitinib significantly increased BA.1 replication in ALI HBE cultures (Figure 2), as indicated by genomic RNA copy numbers (Figure 2B) and cellular NP levels (Figure 2C). In contrast, Delta only displayed a non-significant trend towards higher genomic RNA copy numbers (Figure 2B) and cellular NP levels (Figure 2C) in the presence of baricitinib. Baricitinib did not exert significant effects on BA.1- and Delta-mediated caspase 3/7 activation (Figure 2D) and the ALI HBE barrier function (Figure 2E), although there was a non-significant trend towards enhanced caspase 3/7 activity in BA.1-infected ALI HBE cultures (Figure 2D).

Figure 2

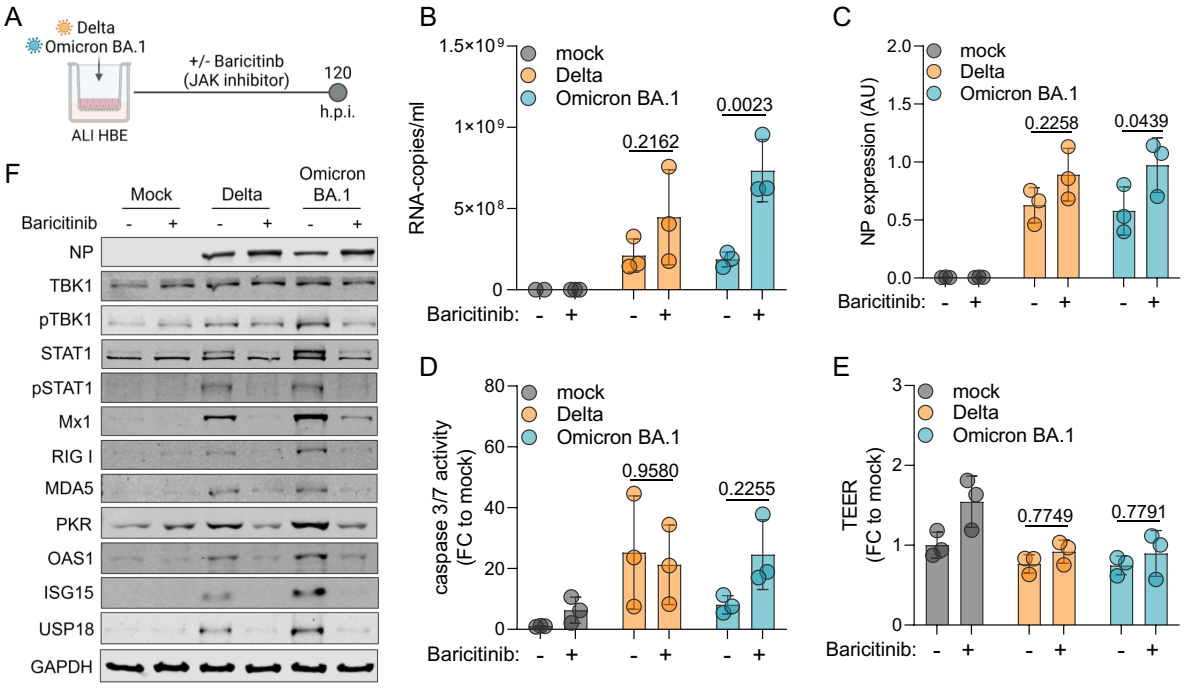

Figure 2. Inhibition of JAK/STAT signalling promotes Omicron BA.1 replication. (A) Schematic depiction of the experimental set-up. (B) SARS-CoV-2 genomic RNA copies in apical wash of air-liquid-interface (ALI) human bronchial epithelial (HBE) cultures 120 h post SARS-CoV-2 (MOI 1) infection in the absence or presence of the JAK inhibitor baricitinib (1µM). Bars represent mean ± SD of three biological replicates. (C) NP levels in SARS-CoV-2 (MOI 1)-infected ALI HBE cultures in the absence or presence of baricitinib (1µM) as determined by immunoblotting. Bars represent mean ± SD of three biological replicates. (D) Caspase 3/7 activation in apical washes of SARS-CoV-2 (MOI 1)-infected ALI HBE cultures in the absence or presence of baricitinib (1µM) 120h post infection. Bars display mean ± SD of three biological replicates. (E) Barrier integrity in SARS-CoV-2 (MOI 1)-infected ALI HBE cultures in the absence or presence of baricitinib (1µM) measured by TEER at 120h post infection. Mean ± SD of three biological replicates is presented. (F) Immunoblot indicating cellular levels of proteins involved in interferon signalling in SARS-CoV-2 (MOI 1)-infected ALI HBE cultures at 120h post infection in the presence or absence of baricitinib (1µM). All P values were calculated by Student´s t-test.

Western blot analysis confirmed that baricitinib not only increased BA.1 replication but also suppressed BA.1-induced interferon signalling (Figure 2F). Taken together, these findings indicate that the pronounced interferon response induced by BA.1 is mediated via STAT1 and that it attenuates BA.1 replication.

BA.1-induced interferon signalling protects air-liquid-interface (ALI) human bronchial epithelial (HBE) cell cultures from H1N1 influenza A virus super-infection

Next, we here infected ALI HBE cultures with BA.1 or Delta (both MOI 1) for 48h prior to infection with H1N1 influenza A virus (MOI 2) (Figure 3A) to examine whether the BA.1-induced interferon response may induce an antiviral state that interferes with H1N1 replication. Controls confirmed that both BA.1 and Delta replication as well as BA.1- and Delta-induced interferon induction were comparable to the data presented in Figure 1 (Suppl. Figure 1).

Figure 3

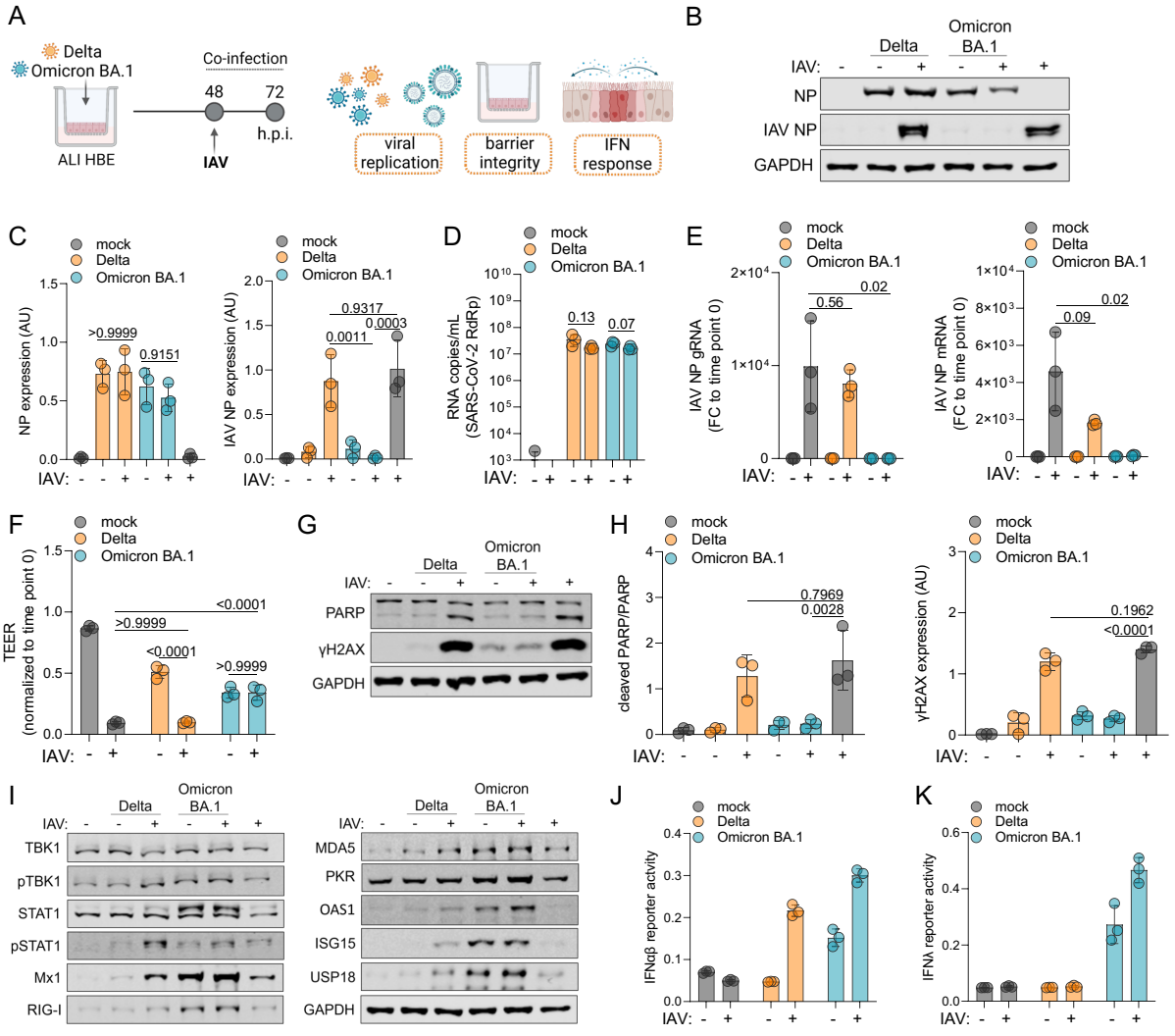

Figure 3 Omicron BA.1 but not Delta infection prevents H1N1 influenza A virus (IAV) replication. (A) Schematic of the experimental set-up. (B) Immunoblot of the SARS-CoV-2 nucleoprotein (NP) and H1N1 IAV NP levels 24 h post infection with H1N1 strain A/NewCaledonia/20/99 (MOI 2). (C) Quantification of immunoblots from (B). Bars represent mean ± SD of three biological replicates. P values were calculated by two-way ANOVA. (D) Genomic RNA copies of the SARS-CoV-2 RNA-dependent RNA polymerase (RdRp) in the apical wash of ALI HBE cultures 24 hours post infection with H1N1 (MOI 2). Values represent means ± SD of three biological replicates. P values were determined by Student´s t-test. (E) IAV NP genomic RNA (gRNA, left) or mRNA (right) levels 24h post infection with H1N1 (MOI 2). Bars display means ± SD of three biological replicates. P values were determined by Student´s t-test. (F) Barrier integrity measure by transepithelial electric resistance (TEER) in single- or co-infected ALI cultures. Bars display means ± SD of three biological replicates. P values were calculated by two-way ANOVA. (G) Immunoblot of PARP cleavage and γH2AX after single- or co-infection. (H) Quantification of the immunoblots from (G). Values represent the mean ± SD of three biological replicates. P values were calculated by two-way ANOVA. (I) Immunoblots displaying the levels of proteins involved in interferon signalling in single- and co-infected ALI HBE cultures. (J, K) Interferon (IFN)α/β (J) or IFNλ (K) signalling in HEK-reporter cell lines incubated with apical washes of single- and co-infected ALI HBE cultures 24 hours post infection with H1N1 (MOI 2).

Determination of H1N1 nucleoprotein (NP) levels indicated that only BA.1 but not Delta suppressed H1N1 infection in ALI HBE cultures (Figure 3B, Figure 3C).

H1N1 super-infection did not significantly reduce SARS-CoV-2 levels in ALI HBE cultures (Figure 3D).

Genomic H1N1 NP RNA and H1N1 NP mRNA levels confirmed that only BA.1 caused a significant reduction of H1N1 replication (Figure 3E). Moreover, only BA.1 infection prevented H1N1-induced cytotoxicity as indicated by transepithelial electric resistance (TEER) measurement (Figure 3F). Influenza A virus replication is associated with the induction of apoptosis and DNA damage induction in host cells [Li et al., 2015; Ampomah & Lim, 2020], and PARP cleavage and γH2AX levels also confirmed that BA.1 infection suppressed H1N1-induced cytotoxicity (Figure 3G, Figure 3H).

The analysis of proteins involved in interferon signalling showed that also in the presence of H1N1 only BA.1 induced a pronounced interferon response (Figure 3I). In agreement, only BA.1-infected (but not of Delta-infected) ALI HBE cultures produced biologically active type I (α/β) and III (λ) interferons, as demonstrated using HEK-reporter cell lines (Figure 3J, Figure 3K). Taken together, these findings indicate that only BA.1 but not Delta induces an interferon-mediated antiviral state in ALI-HBE cultures that protects them from H1N1 infection.

Inhibition of JAK/ STAT signalling promotes H1N1 influenza A virus replication in BA.1-infected cells

Next, we investigated the effect of the JAK inhibitor on the BA.1-mediated suppression of H1N1 replication (Figure 4A). In agreement with the data presented in Figure 2 and Figure 3, baricitinib increased BA.1 replication as indicated by genomic RNA copies of the viral RNA-dependent RNA polymerase gene (Figure 4B). Moreover, baricitinib prevented the BA.1-mediated inhibition of H1N1 replication as indicated by

232 H1N1 NP mRNA and genomic RNA levels (Figure 4C) and H1N1 NP protein levels
233 (Figure 4D, Figure 4E).

234 In line with our previous findings, baricitinib also antagonised BA.1-induced
235 suppression of H1N1-induced apoptosis as indicated by PARP cleavage and H1N1-
236 induced DNA damage as indicated by cellular γH2AX levels (Figure 4F, Figure 4G).
237 Furthermore, baricitinib abrogated the BA.1-mediated protection of the ALI HBE
238 barrier integrity from H1N1-induced cytotoxicity (Suppl. Figure 2).
239

Figure 4

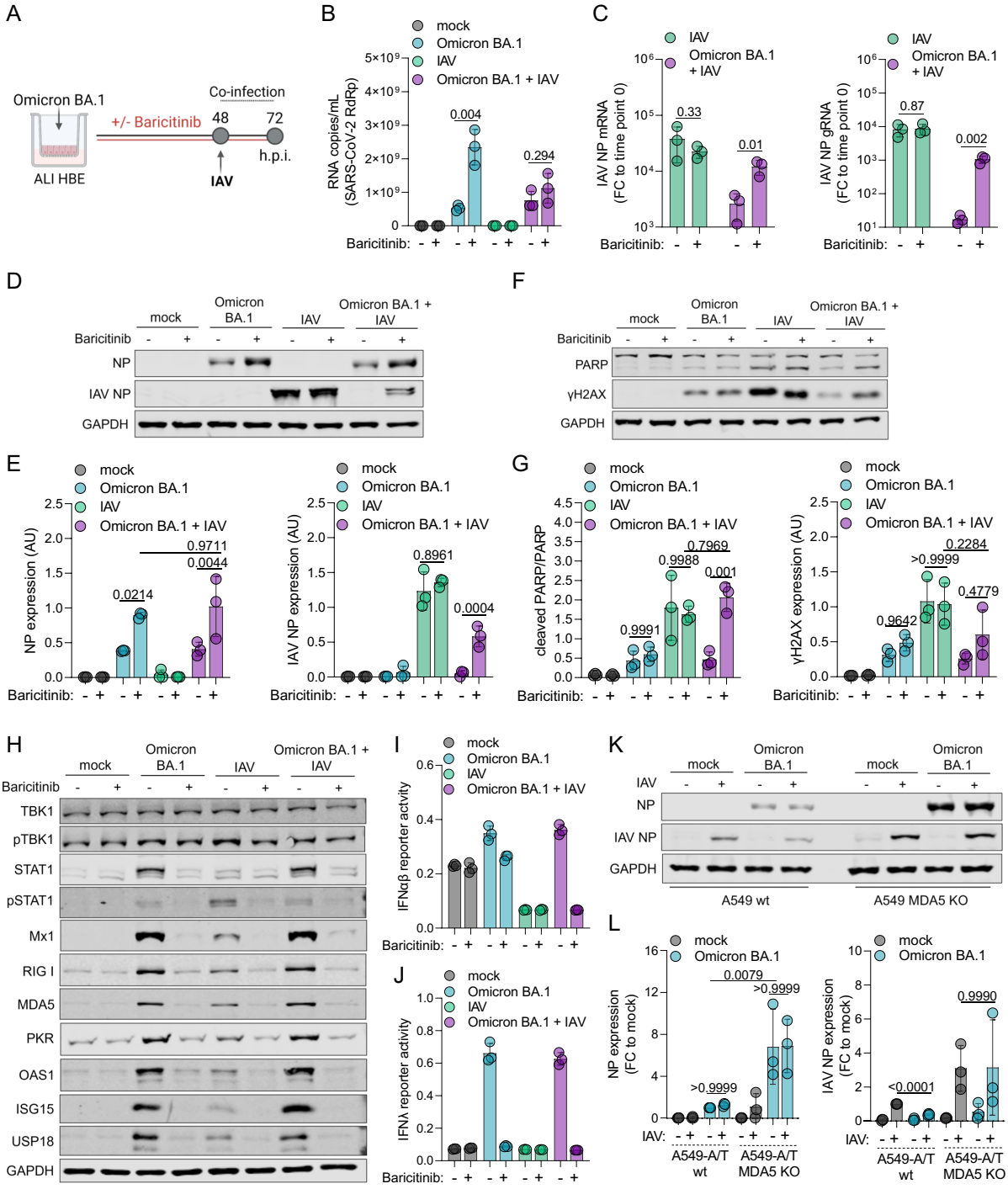

Figure 4. Inhibition of JAK/ STAT signalling prevents Omicron BA.1-mediated suppression of H1N1 influenza A virus (IAV) replication in air-liquid-interface (ALI) human bronchial epithelial (HBE) cultures. (A) Experimental set-up. (B) Genomic RNA copy numbers (RNA-dependent RNA polymerase gene = RdRp) in apical washes of BA.1 (MOI 1)-infected ALI HBE cultures 72h post infection in the

absence or presence of baricitinib 1µM. Values represent mean ± SD of three biological replicates. P values were determined by Student´s t-test. (C) IAV NP mRNA (left) or genomic RNA (right) levels 24h post H1N1 (MOI 2) infection in the absence or presence of baricitinib 1µM. Bars represent mean ± SD of three biological replicates. P values were determined by Student´s t-test. (D) Immunoblot indicating BA.1 NP and IAV NP protein levels 72 h post BA.1 infection in the absence or presence of baricitinib 1µM. (E) Quantification of the immunoblot results from (D) by ImageJ. Values represent mean ± SD of three biological replicates. P values were calculated by two-way ANOVA. (F) Immunoblot indicating PARP cleavage and γH2AX protein levels 72 h post BA.1 infection in the absence or presence of baricitinib 1µM. (G) Quantification of the immunoblot results from (F) by ImageJ. Bars represent the quantification of the ratio between cleaved and total PARP (left) and cellular γH2AX levels (right). Values represent mean ± SD of three biological replicates. P values were calculated by two-way ANOVA. (H) Immunoblot displaying levels of proteins involved in interferon signalling in single- and co-infected ALI HBE cultures in the absence or presence of baricitinib 1µM. (I, J) Interferon (IFN)α/β (I) or -λ (J) activity in HEK reporter cell lines incubated with apical washes of ALI HBE cultures 72h post infection. (K) BA.1 NP and IAV NP protein levels in ACE2/ TMPRSS2-transduced A549 (A549-A/T) cells (A549-A/T wt) or A549-A/T MDA5 knock-out (KO) cells infected with BA.1 at MOI 0.01 for 24h and followed by influenza A virus (IAV) H1N1 (MOI 2) infection for an additional 24h. (L) Quantification of immunoblot results from (K) by ImageJ. Values represent the mean ± SD of three biological replicates. P values were calculated by two-way ANOVA.

As indicated by the cellular levels of proteins involved in interferon signalling, the BA.1-induced interferon was not affected by of H1N1 (Figure 4H). Moreover, baricitinib inhibited interferon signalling in response to ALI HBE infection with either single virus and after co-infection with both viruses (Figure 4H) and suppressed interferon-α/β and -λ production (Figure 4I, Figure 4J).

The pattern recognition receptor MDA5 was previously shown to be critically involved in the SARS-CoV-2-mediated, and in particular the BA.1-mediated, interferon response [Yin et al., 2021; Bojkova et al., 2022; Bojkova et al., 2022a]. In agreement, BA.1-mediated inhibition of H1N1 infection was abrogated in MDA5 knock-out cells (Figure 4K, Figure 4L).

Taken together, our data show that BA.1-mediated suppression of H1N1 replication depends on the presence of MDA5 and is anatagonised by inhibition of JAK/ STAT signalling by baricitinib.

Similar suppression of H1N1 influenza A virus replication by BA.1 and BA.5

Next, we compared the effects of BA.1 on interferon signalling and H1N1 replication to those of the Omicron subvariant BA.5 (Figure 5A), which is currently dominant in many parts of the world [Shrestha et al., 2022].

BA.1 and BA.5 infection of ALI HBE cultures resulted in similar SARS-CoV-2 NP protein levels (Figure 5B, Figure 5C) and induced similar interferon responses as indicated by the cellular levels of the interferon-stimulated gene products MX1 and ISG15 (Figure 5B) as well as interferon-α/β (Figure 5D) and -λ (Figure 5E) production in BA.1- and BA.5-infected ALI HBE cultures.

Figure 5

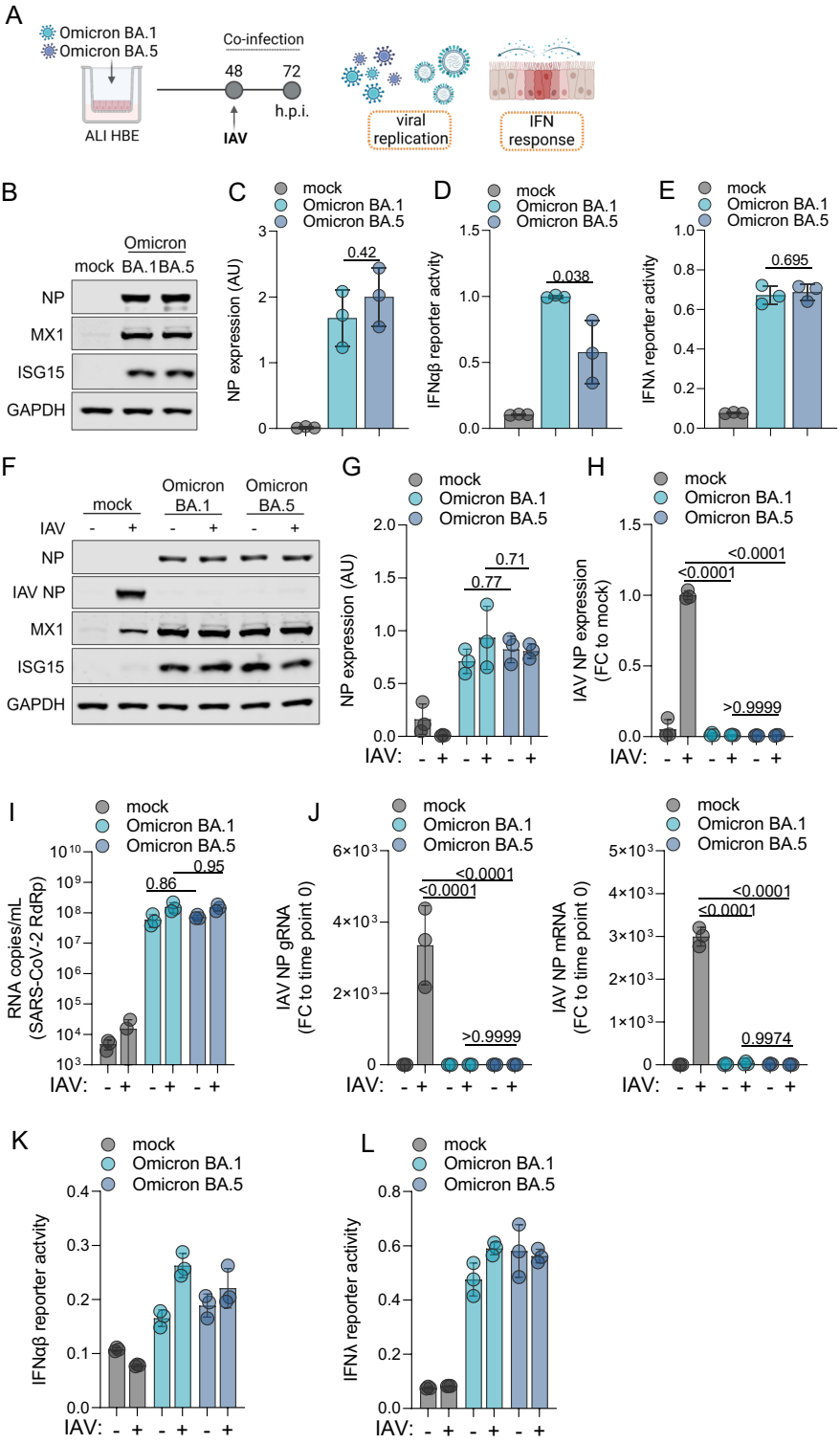

Figure 5. Effects of Omicron BA.1 and BA.5 on interferon signalling and H1N1 influenza A virus replication in air-liquid-interface (ALI) human bronchial epithelial (HBE) cell cultures. (A) Experimental design. (B) Cellular levels of the

SARS-CoV-2 nucleoprotein (NP) and proteins involved in interferon signalling (MX1, ISG15) in BA.1- and BA.5 (MOI 1)-infected ALI HBE cultures 48h post infection. (C) Quantification of the NP immunoblot results from (B). Values represent mean ± SD from three biological replicates. P values were determined by Student's t-test. (D,E) Interferon-α/β (D) or -λ (E) promotor activity in HEK reporter cell lines incubated with apical washes of BA.1- or BA.5-infected ALI HBE cultures 48h post infection. (F) SARS-CoV-2 NP (NP), influenza A virus NP (IAV NP), MX1, and ISG15 protein levels in BA.1 (MOI 1)-infected, BA.5 (MOI 1)-infected, IAV H1N1 (MOI 2)-infected, BA.1/ IAV co-infected, or BA.5/ IAV co-infected ALI HBE cultures. (G,H) Quantification of SARS-CoV-2 NP (G) and IAV NP (H) levels from (F) by ImageJ. (I) Genomic SARS-CoV-2 RNA (RNA-depended RNA polymerase/ RdRp gene) levels in BA.1-infected, BA.5-infected, BA.1/ IAV co-infected, and BA.5/ IAV co-infected cells 72h post infection. Values represent mean ± SD from three biological replicates. (J) Genomic IAV NP (gRNA) copy numbers and IAV NP mRNA levels in BA.1-infected, BA.5-infected, BA.1/ IAV co-infected, and BA.5/ IAV co-infected cells 72h post infection. (K, L) Interferon-α/β (K) or -λ (L) promotor activity in HEK reporter cell lines incubated with apical washes of BA.1-infected, BA.5-infected, BA.1/ IAV co-infected, and BA.5/ IAV co-infected ALI HBE cultures 72h post infection.

H1N1 co-infection did not significantly affect cellular SARS-CoV-2 NP levels or cellular MX1 and ISG15 levels (Figure 5F, Figure 5G). However, both Omicron subvariants suppressed H1N1 replication as indicated by cellular NP levels (Figure 5F, Figure 5H). These findings (limited impact of influenza A virus infection on SARS-CoV-2 replication, BA.1- and BA.5-mediated suppression of H1N1 replication) were confirmed by the determination of genomic SARS-CoV-2 RNA copy numbers (Figure

5I), genomic influenza A virus RNA copy numbers (Figure 5J), and H1N1 NP mRNA levels (Figure 5J). Both variants also induced similar interferon responses in the presence or absence of H1N1 as indicated by interferon-α/β (Figure 5K) and -λ (Figure 5L) production.

Taken together, BA.1 and BA.5 induce comparable interferon-mediated antiviral states in ALI HBE cultures that prevent H1N1 replication.

BA.1-induced interferon signalling prevents H1N1 and H5N1 influenza A virus replication in primary human monocytes

Influenza A viruses can replicate in peripheral blood mononuclear cells, including CD14+ monocytes [Lersritwimanmaen et al., 2015; Lee et al., 2017], and interferon signalling in monocytes has been suggested to be a critical determinant of influenza A virus pathogenesis [Hartshorn, 2020; Fourati et al., 2022]. Highly pathogenic avian influenza A H5N1 virus has been described to replicate more readily in monocytes and macrophages than H1N1 [Yu et al., 2011; Hoeve et al., 2012; Cline et al., 2017; Lee et al., 2017; Lamichhane & Puthavathana, 2018; Lamichhane et al., 2018; Westenius et al., 2018]. Hence, we finally investigated the impact of BA.1 and Delta on H1N1 and H5N1 virus infection in primary human monocytes (Figure 6A).

The determination of SARS-CoV-2 E mRNA levels by quantitative PCR showed that BA.1 and Delta did not replicate in primary human monocytes (Figure 6B), which confirmed previous findings showing that SARS-CoV-2 causes abortive infections in monocytes [McLaughlin et al., 2021; Junqueira et al., 2022]. Only BA.1 induced a pronounced interferon response as indicated by interferon α/β signalling in a HEK reporter cell line incubated with supernatants from infected monocytes (Figure 6C), MX1 mRNA levels, and ISG15 mRNA levels (Figure 6D). In contrast to the findings in

348 ALI HBE cultures (Figure 1H, Figure 2K, Figure 4J, Figure 5L), supernatants from
349 BA.1-infected monocytes did not induce interferon-λ activity in a HEK reporter cell line
350 (Figure 6C).

Figure 6

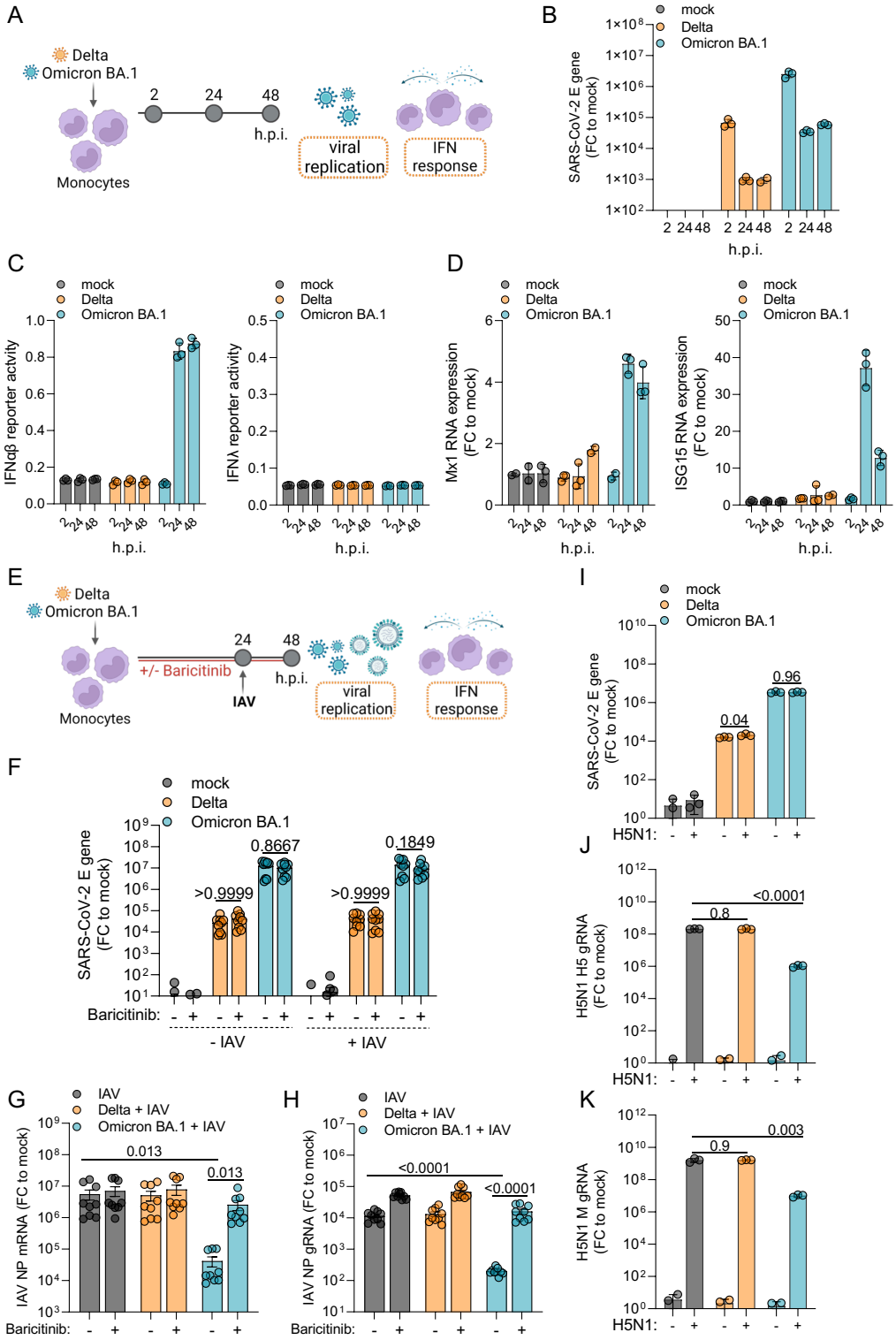

351

Figure 6. Impact of Omicron BA.1 and Delta on H1N1 and H5N1 influenza A virus (IAV) infection of primary human monocytes. (A) Experimental design underlying (B-D). (B) SARS-CoV-2 E gene expression levels as determined by quantitative PCR. Values represent mean ± SD of three biological replicates. (C) interferon-α/β (IFNα/β) (left) or IFNλ (right) activity induced by supernatants of Delta and BA.1 (MOI 1)-infected primary human monocytes in HEK-reporter cell lines. (D) Mx1 (left) and ISG15 (right) mRNA levels in Delta and BA.1 (MOI 1)-infected primary human monocytes as indicated by quantitative PCR. (E) Experimental design underlying (F-H). (F) SARS-CoV-2 E mRNA levels in monocytes infected with Delta (MOI 1), BA.1 (MOI 1), Delta plus H1N1 IAV (MOI 2), or BA.1 plus H1N1 IAV (MOI 2) in the absence or presence of baricitinib 1μM. P values were determined by Student´s t-test. (G, H) H1N1 IAV NP mRNA (G) or genomic mRNA (H) levels in monocytes infected with Delta (MOI 1), BA.1 (MOI 1), Delta plus H1N1 IAV (MOI 2), or BA.1 plus H1N1 IAV (MOI 2) in the absence or presence of baricitinib 1μM 24h post H1N1 IAV infection. P values were calculated by two-way ANOVA. (I-K) Impact of BA.1 and Delta infection on highly pathogenic avian H5N1 IAV virus infection in monocytes. SARS-CoV-2 genomic E RNA levels (I), genomic H5N1 H5 RNA levels (J), and genomic H5N1 IAV M levels (K) in monocytes infected with Delta (MOI 1), BA.1 (MOI 1), Delta plus H5N1 strain A/Vietnam/1203/04 (MOI 1), or BA.1 plus H5N1 (MOI 1). P values were calculated by two-way ANOVA. All values represent mean ± SD of monocyte preparations derived from three different donors (A-H) or one donor (I-K), which were each tested in three biological replicates.

Next, we tested the impact of BA.1 and Delta on H1N1 replication in primary human monocytes in the absence or presence of the JAK inhibitor baricitinib (Figure

6E). Neither baricitinib nor H1N1 infection affect SARS-CoV-2 E mRNA levels (Figure 6F).

Similarly as in ALI HBE cultures, however, BA.1 (but not Delta) infection reduced H1N1 infection as indicated by H1N1 NP mRNA (Figure 6G) and H1N1 genomic NP RNA levels (Figure 6H), which was prevented by baricitinib (Figure 6G, Figure 6H).

Highly pathogenic H5N1 avian influenza A virus also did not affect SARS-CoV-2 levels in monocytes as indicated by SARS-CoV-2 genomic E RNA levels (Figure 6I). However, the determination of H5N1 virus genomic H5 (Figure 6J) and M (Figure 6K) levels showed that abortive BA.1 but not Delta infection inhibited H5N1 replication in primary human monocytes.

Taken together, abortive BA.1 but not Delta infection induced an interferon response and reduced H1N1 and H5N1 replication in monocytes. The JAK/ STAT inhibitor prevented BA.1-mediated H1N1 and H5N1 inhibition in monocytes, indicating that BA.1-mediated influenza A virus inhibition is caused by BA.1-induced interferon signalling.

Comparison of the circulation of influenza-like illnesses during the Delta and BA.1 infection waves in England

An analysis comparing the spread of influenza-like illnesses (includes cases of clinically diagnosed influenza with or without a virus test confirmation) and COVID-19 in England showed that both Delta and influenza-like illnesses surged after all restrictions were removed on 19th July 2021. When BA.1 became the dominant variant, however, the number of influenza-like illnesses strongly declined and has not surged since (Suppl. Figure 3). These data fit with our findings showing that BA.1 but not Delta

induces an interferon response that prevents influenza A virus infection. Similarly, an analysis of data from the John Hopkins Microbiology Laboratory found a notable decrease in influenza A virus infections during the Omicron BA.1 wave between November 2021 and February 2022 [Eldesouki et al., 2022]. However, future research will have to analyse a possible causative relationship in more detail.

Discussion

Here, we investigated the impact of Delta and the Omicron subvariants BA.1 and BA.5 on interferon signalling in ALI HBE cultures and primary human monocytes. Our results consistently showed that only Omicron causes pronounced production of biologically active type I and type III interferons (Suppl. Figure 4). The kinetics of the interferon type I (α/β) and type III (λ) responses provided additional mechanistic evidence explaining the reduced pathogenicity of Omicron relative to Delta [Wang et al., 2022]. BA.1 infection caused an early, transient interferon-α/β peak, which is anticipated to mediate a protective antiviral response but also to avoid deleterious inflammatory processes associated with prolonged interferon type I activation [Forero et al., 2019; King & Sprent, 2021]. Moreover, BA.1 infection caused a sustained interferon λ response known to inhibit virus replication and prevent excessive inflammation in the respiratory tract [Forero et al., 2019; Prokunina-Olsson et al., 2020; King & Sprent, 2021].

The Omicron-induced interferon response generated an antiviral state that protected infected cells from super-infection with influenza A viruses, showing that the Omicron-induced interferon response is of functional relevance. Our analysis of the spread of influenza-like illnesses during the Delta and BA.1 infection waves (Suppl. Figure 3) and data from the John Hopkins Microbiology Laboratory [Eldesouki et al., 2022] found that the levels of influenza A virus transmission levels strongly declined with the emergence of BA.1, but a causative relationship remains to be established.

Despite consistent BA.1-mediated interferon induction across the different cell types, the relative replication kinetics of Omicron and Delta differed between the models. BA.1 replicated less effectively than Delta in Caco-2F03 and Calu-3 [Bojkova et al., 2022; Bojkova et al., 2022a], but (in agreement with other findings [Hui et al.,

2022]) faster than Delta in ALI HBE cultures. This probably reflects the contribution of many factors to SARS-CoV-2 replication. The spike (S) proteins of the BA.1 and Delta isolates that we used differ in 13 amino acid positions in the S receptor binding domain (Suppl. Figure 5). For example, BA.1 S is known to interact differently with its cellular receptor ACE2, to utilise ACE2 from a broader range of species as receptor, and to mediate increased virus uptake [Cameroni et al., 2022; Hong et al., 2022; Li et al., 2022; Meng et al., 2022; Rathnasinge et al., 2022; Willett et al., 2022; Zhang et al., 2022].

Increased BA.1 uptake may also contribute to the enhanced interferon response. Mechanistically, the BA.1-induced interferon response is, in agreement with previous studies in other cell types [Yin et al., 2021; Bojkova et al., 2022; Bojkova et al., 2022a], primarily mediated by the recognition of double-stranded RNA by the pattern recognition receptor MDA5, as suggested by the lack of a BA.1-induced interferon in MDA5 knock-out cells. In this context, virus uptake via the endosomal pathway was described to result in greater activation of pattern recognition receptors [Peacock et al., 2022].

BA.1 infection also induced an interferon-mediated antiviral state preventing influenza A (H1N1, H5N1) infection in monocytes despite only establishing an abortive infection, demonstrating that the antiviral state does not depend on a complete virus replication cycle resulting in the production of infectious virus. In agreement, UV-inactivated BA.1 had previously been shown to trigger a detectable interferon response in lung organ cultures, although this response was weaker than that induced by the replication-competent virus [Alfi et al., 2022].

The JAK/ STAT inhibitor baricitinib inhibited the Omicron-mediated antiviral response. This suggests that the Omicron-induced antiviral state is caused by MDA5-

460 mediated production of interferon which activates interferon receptors that then trigger
461 JAK/ STAT signalling [Li et al., 2020].

462 In addition to these findings, we also showed that BA.5, which is currently the
463 dominant variant in many parts of the world [Shrestha et al., 2022], induces a
464 comparable interferon response to BA.1 and that the BA.1- and BA.5-induced
465 interferon responses protect infected cells from super-infection with influenza A
466 viruses. The latter finding demonstrates that the BA.1- and BA.5-induced interferon
467 signalling is of functional relevance. Baricitinib prevented the BA.1- and BA.5-induced
468 suppression of influenza A virus replication, providing evidence that the BA.1- and
469 BA.5-induced interferon response is responsible for the BA.1 and BA.5-induced
470 influenza A virus inhibition.

471 In summary, we show that BA.1 and BA.5 (but not Delta) induce a functionally
472 relevant pronounced interferon response that suppresses influenza A virus replication.
473 Further research will have to show the relevance of our findings in the context of
474 SARS-CoV-2/ influenza virus co-infection. Data on the severity of SARS-CoV-2/
475 influenza A virus co-infections are inconsistent in cell culture and animal models
476 [Andrés et al., 2022; Kim EH et al., 2022; Kim HK et al., 2022; Oishi et al., 2022] and
477 in humans [Cuadrado-Payán et al., 2020; Yue et al., 2020; Alosaimi et al., 2021; Stowe
478 et al., 2021; Xiang et al., 2021; Krumbein et al., 2022; Swets et al., 2022]. This may
479 not be a surprise, given the differences in interferon signalling between different
480 SARS-CoV-2 variants that we present here and that were described in previous
481 studies [Alfi et al., 2022; Bojkova et al., 2022; Bojkova et al., 2022a; Guo et al., 2022;
482 Thorne et al., 2022]. Future studies may have to include more different virus variants
483 and strains to establish a clearer picture.

484 In conclusion, our findings show that 1) BA.1 and BA.5 induce comparable
485 interferon responses in ALI HBE cultures, 2) the Omicron-induced interferon-response
486 is of functional relevance as it protects infected cells from influenza A virus replication,
487 and 3) abortive BA.1 infection of monocytes is sufficient to produce a protective
488 interferon response. Moreover, the kinetics of the Omicron-induced interferon
489 response (early and transient type I response, sustained type III response) provide
490 additional mechanistic evidence explaining why Omicron infections are usually
491 associated with less severe disease than Delta infections.
492

Methods

Cell lines

HEK293 (HEK-Blue™ reporter cells, InvivoGen) -IFN-α/β and -IFN-λ cells were cultivated in DMEM (Gibco, ThermoFisher Scientific) with 10% heat-inactivated foetal bovine serum (Sigma), Pen-Strep (100 U/ml-100 µg/ml) (Sigma), 100 µg/ml Normocin™ (InvivoGen) and the required selective antibiotic for each cell line (IFN-α/β: Blasticidin and Zeocin; IFN-λ, Blasticidin, Puromycin, and Zeocin) at 37°C and 5% CO_2.

A549-ACE2/TMPRSS2 cells (Invivogen) were grown in DMEM supplemented with 2 mM L-glutamine, 4.5 g/l glucose, 10% (v/v) heat-inactivated fetal bovine serum (FBS; 30 min at 56 ºC), PenStrep (100 U/ml-100 µg/ml), 100 µg/ml Normocin, 10 µg/ml of Blasticidin, 10 µg/ml of Blasticidin, 100 µg/ml of Hygromycin, 0.5 µg/ml of Puromycin, and 100 µg/ml of Zeocin. A549-ACE2/TMPRSS2 MDA5 KO cells (Invivogen) were grown in DMEM supplemented with 2 mM L-glutamine, 4.5 g/l glucose, 10% (v/v) heat-inactivated fetal bovine serum (FBS; 30 min at 56 ºC), PenStrep (100 U/ml-100 µg/ml), 100 µg/ml Normocin, 10 µg/ml of Blasticidin, 100 µg/ml of Hygromycin, 0.5 µg/ml of Puromycin, and 100 µg/ml of Zeocin.

All cell lines were regularly tested for mycoplasma contamination.

Air-liquid interface cultures

Lung tissue for the isolation of primary epithelial cells was provided by the Hannover Medical School, Institute of Pathology (Hannover, Germany). The use of tissue was approved by the ethics committee of the Hannover Medical School (MHH, Hannover, Germany, number 2701–2015) and was in compliance with The Code of Ethics of the World Medical Association. Primary bronchial epithelial cells were isolated from the

lung explant tissue of a patient with lung emphysema as described previously [van Wetering et al., 2000]. All patients or their next of kin gave written informed consent for the use of their lung tissue for research.

Basal cells were expanded in Keratinocyte-SFM medium supplemented with bovine pituitary extract (25 µg/mL), human recombinant epidermal growth factor (0.2 ng/mL, all from Gibco, Schwerte, Germany), isoproterenol (1 nM, Sigma), Antibiotic/Antimycotic Solution (Sigma-Aldrich), and MycoZap Plus PR (Lonza, Cologne, Germany) and cryopreserved until further use.

For differentiation, the cells were thawed and passaged once in PneumaCult-Ex Medium (StemCell Technologies, Cologne, Germany) and then seeded on transwell inserts (12-well plate, Sarstedt, Nümbrecht, Germany) at 4×10^4 cells/insert. Once the cell layers reached confluency, the medium on the apical side of the transwell was removed, and medium in the basal chamber was replaced with PneumaCult ALI Maintenance Medium (StemCell Technologies), including Antibiotic/Antimycotic Solution (Sigma-Aldrich) and MycoZap Plus PR (Lonza). During a period of four weeks, the medium was changed and the cell layers were washed with PBS every other day. Criteria for successful differentiation were the development of ciliated cells and ciliary movement, an increase in transepithelial electric resistance indicative of the formation of tight junctions, and mucus production.

SARS-CoV-2 variants preparation

The SARS-CoV-2 isolates Omicron BA.1 (B.1.1.529: FFM-SIM0550/2021, EPI_ISL_6959871, GenBank ID OL800702), Delta (B.1.167.2: FFM-IND8424/2021, GenBank ID MZ315141), and Omicron BA.5 (GenBank ID OP062267) were isolated in Caco-2-F03 cells as previously described [Cinatl et al., 2004; Bojkova et al., 2021]

and stored at –80°C. All variants underwent maximum two passages. Virus titres were determined as TCID50/mL.

Influenza A virus strains H1N1 and H5N1

The H1N1 influenza strain A/NewCaledonia/20/99 was received from the World Health organisation (WHO) Influenza Centre (National Institute for Medical Research, London, UK) and stocks were prepared by cultivation on MDCK cells (ATCC, CCL-34) in medium containing 2µg/ml trypsine. Virus stocks were stored at −80 °C. Virus titres were determined as TCID50/mL.

The H5N1 influenza strain A/Vietnam/1203/04 was received from the World Health organisation (WHO) Influenza Centre (National Institute for Medical Research, London, UK). Virus stocks were prepared by infecting Vero cells, and aliquots were stored at −80 °C. Virus titres were determined as TCID50/mL.

Barrier integrity measurement

For trans-epithelial electrical resistance (TEER) measurement, medium was added to the apical side 30min prior to measurement with a chopstick electrode connected to a Volt-Ohm-meter (Millicell® ERS-2, Merck, Darmstadt, Germany) according to the manufacturer's instructions. Blank inserts served as baseline. The apical medium was removed after the measurement.

Activation of caspase 3/7

Caspase 3/7 activity was measured using the Caspase-Glo assay kit (Promega, Madison, WI, USA), according to the manufacturer's instructions. Briefly, 100 µL of Caspase-Glo reagent were added to each well containing 100 µL of tested

sample, mixed, and incubated at room temperature for 30 min. Luminescence intensity was measured using an Infinite M200 microplate reader (Tecan).

Co-infection assay in ALI HBE

ALI HBE cultures were infected with SARS-CoV-2 variant at MOI 1 from the apical site. The inoculum was incubated for 2 h, then removed and cells were washed three times with PBS. H1N1 A/NewCaledonia/20/99 at MOI 2 was added 48 h post SARS-CoV-2 infection. The inoculum was incubated for 2 h, then removed and cells were washed three times with PBS.

Detection of extracellular and intracellular RNA

SARS-CoV-2 RNA from the apical washes of the ALI HBE culture was isolated using QIAamp Viral RNA Kit (Qiagen, Hilden, Germany) according to the manufacturer's instructions. RNA was subjected to OneStep qRT-PCR analysis using the Luna Universal One-Step RT-qPCR Kit (New England Biolabs, Frankfurt am Main, Germany) and a CFX96 Real-Time System, C1000 Touch Thermal Cycler (Bio-Rad, Feldkirchen, Germany). Primers were adapted from the WHO protocol29 targeting the open reading frame for RNA-dependent RNA polymerase (RdRp): RdRP_SARSr-F2 (GTG ARA TGG TCA TGT GTG GCG G) and RdRP_SARSr-R1 (CAR ATG TTA AAS ACA CTA TTA GCA TA) using 0.4 µM per reaction. Standard curves were created using plasmid DNA (pEX-A128-RdRP) as previously described [Bojkova et al., 2020].

Intracellular RNA isolation was carried out according to manufacturer's protocol (RNeasy 96 QIAcube HT Kit, Qiagen, Hilden, Germany). Detection of selected targets was performed with Luna® Universal One-Step RT-qPCR (New England BioLabs Inc.) according to manufacturers protocol using specific primers: TBP (fw:5′-

ATCAGAACAACAGCCTGCC-3′; rev: 5′- GGTCAGTCCAGTGCCATAAG-3′); SARS-CoV-2 E gene (fw:5′- ACAGGTACGTTAATAGTTAATAGCGT-3′; rev:5′-ATATTGCAGCAGTACGCACACA-3′); ISG15 (fw:5′-GAGAGGCAGCGAACTCATCT-3′; rev:5′-AGGGAC ACCTGGAATTCGTT-3′); MX1 (fw:5′-TTTTCAAGAAGGAGGCCAGCAA-3′; rev:5′-TCAGGAACTTCCGCTTGTCG-3′); H5N1 H5 gene (fw:5′-GCCATTCCACAACATACACCC-3′; rev:5′-CTCCCCTGCTCATTGCTATG-3′); H5N1 M gene (fw:5′-TTCTAACCGAGGTCGAAACG-3′; rev:5′-ACAAAGCGTCTACGCTGCAG-3′); IAV NP-mRNA (fw:5′- GACTCACATGATGATCTGGCA-3′; rev:5′-CTTGTTCTCCGTCCATTCTCA-3′); IAV NP-gRNA (fw:5′-AACGGCTGGTCTGACTCACATGAT-3′; rev:5′-AGTGAGCACATCCTGGGATCCATT-3′).

Immunoblot analysis

Whole-cell lysates were prepared using Triton-X sample buffer containing protease inhibitor cocktail (Roche). The protein concentration was assessed by using DC Protein assay reagent (Bio-Rad Laboratories). Equal protein loads were separated by sodium dodecyl sulfate-polyacrylamide gel electrophoresis and proteins were transferred to nitrocellulose membranes (Thermo Scientific). For protein detection the following primary antibodies were used at the indicated dilutions: GAPDH (Cell Signaling, #2118, 1:4000), γH2AX (Cell Signaling, #9718, 1:1000), H1N1 (Influenza A Virus) Nucleoprotein (Bioss, #bs-4976R, 1:4000), ISG15 (Santa Cruz Biotechnology, #sc-166755, 1:200), MDA5 (Cell Signaling, #5321, 1:1000), Mx1 (Cell Signaling, #37849, 1:1000), OAS1 (Cell Signaling, #14498, 1:1000), PARP (Cell Signaling, #9542, 1:1000), PKR (Cell Signaling, #12297, 1:1000), SARS-CoV-2 Nucleocapsid

(Sino Biological, #40143-R019, 1:10000), STAT1 (Cell Signaling, #9172, 1:1000), phospho-STAT1 Y701 (Cell Signaling, #9171, 1:1000), TBK1 (Cell Signaling, #3013, 1:1000), phospho-TBK1 S172 (Cell Signaling, #5483, 1:1000), USP18 (Cell Signaling, #4813, 1:2000) and RIG1 (Cell Signaling, #3743, 1:1000). Protein bands were visualised using IRDye-labeled secondary antibodies at dilution 1:40000 (LI-COR Biotechnology, IRDye®800CW Goat anti-Rabbit, #926-32211 and IRDye®800CW Goat anti-Mouse IgG, #926-32210) and Odyssey Infrared Imaging System (LI-COR Biosciences).

Detection of type I and type III IFNs production

Detection of type I and type III IFNs in supernatants was carried out with HEK-Blue™ IFN-α/β (type I) and HEK-Blue™ IFN-λ (type III) cells according to manufacturer's protocol. HEK cells were washed twice with PBS and detached in presence of PBS by tapping the flask. Cells were subsequently centrifuged at 200g for 5 min and resuspended in Test Medium (DMEM, 4.5 g/l glucose, 2 mM L-glutamine, 10% (v/v) heat-inactivated FBS, 50 U/ml penicillin, 50 µg/ml streptomycin,100 µg/ml Normocin™) at 280.000 cells/ml. 20µl supernatant were added in 96 well plates and 180 µl cell suspension was added to the wells. Cells and supernatant were incubated at 37°C and 5% CO_2 for 24h. After incubation, 20 µl supernatant was removed and incubated with 180 µl QUANTI-Blue™ Solution for 1-3 h. SEAP (secreted embryonic alkaline phosphatase) levels were determined using a spectrophotometer at 620nm.

PBMCS isolation

Human peripheral blood mononuclear cells were isolated from buffy coats of healthy donors (RK-Blutspendedienst Baden-Württemberg-Hessen, Institut für

643 Transfusionsmedizin und Immunhämatologie Frankfurt am Main, Germany). After
644 centrifugation on a Ficoll (Pancoll, PAN-Biotech, Aidenbach, Germany) density
645 gradient, mononuclear cells were collected from the interface, washed with PBS, and
646 plated on cell culture dishes (Cell+, Saarstedt, Nümbrecht, Germany) in RPMI1640
647 (Gibco, ThermoFisher Scientific, Waltham, MA, USA) supplemented with 100 IU/mL
648 penicillin and 100 g/mL streptomycin. After incubation for 90 min(37°C, 5% CO2), non-
649 adherent cells were removed, and the medium was changed to RPMI1640
650 supplemented with 100 IU/mL penicillin, 100 µg/mL of streptomycin, and 3% human
651 serum (RK-Blutspendedienst Baden-Württemberg-Hessen, Institut für
652 Transfusionsmedizin und Immunhämatologie Frankfurt am Main, Germany).
653

654 **Co-infection assay in human PBMCs**

655 Human PBMCs were infected with SARS-CoV-2 variants at MOI of 1 for 2 h in
656 infection medium (RPMI1640 supplemented with 100 IU/mL penicillin and 100 g/mL
657 streptomycin, 1% heat-inactivated fetal bovine serum) at 37°C at 5% CO2. Afterwards
658 the cells were washed twice with PBS and incubated for 24 h in infection medium. For
659 co-infection, the cells were either infected with influenza A virus H1N1/New
660 Caledonia/20/99 (MOI 2), influenza A virus H5N1 A/Vietnam/1203/04 (MOI 1) or
661 treated with medium for 2 h, washed twice and incubated again for 24 h. After each
662 washing step and after 48 h supernatant samples were taken and cells were lysed for
663 RNA isolation.
664

665 **Statistics**

666 Results are expressed as the mean ± standard deviation (SD) of the number of
667 biological replicates indicated in figure legends. Statistical significance is depicted

668 directly in graphs and the statistical tests used for the calculation of p values are
669 indicated in the figure legends. GraphPad Prism 9 was used for visualisation of the
670 data and for calculation of statistical significance.
671

672 **Acknowledgements**

673 We thank Lena Stegman, Kerstin Euler, and Sebastian Grothe for their

674 technical assistance.

675 **Funding**

676 This work was supported by the Frankfurter Stiftung für krebskranke Kinder,

677 the Goethe-Corona-Fonds, and the BMBF (COVID-Protect, FZ: 01KI20143A).

678 **Competing interests**

679 The authors declare no competing interests.

680

681

682 **References**

683 Alfi O, Hamdan M, Wald O, Yakirevitch A, Wandel O, Oiknine-Djian E, Gvili B, Knoller
684 H, Rozendorn N, Golan Berman H, Adar S, Vorontsov O, Mandelboim M, Zakay-
685 Rones Z, Oberbaum M, Panet A, Wolf DG. SARS-CoV-2 Omicron Induces Enhanced
686 Mucosal Interferon Response Compared to other Variants of Concern, Associated
687 with Restricted Replication in Human Lung Tissues. Viruses. 2022 Jul 21;14(7):1583.
688 doi: 10.3390/v14071583.

689 Alosaimi B, Naeem A, Hamed ME, Alkadi HS, Alanazi T, Al Rehily SS, Almutairi AZ,
690 Zafar A. Influenza co-infection associated with severity and mortality in COVID-19
691 patients. Virol J. 2021 Jun 14;18(1):127. doi: 10.1186/s12985-021-01594-0.

692 Ampomah PB, Lim LHK. Influenza A virus-induced apoptosis and virus propagation.
693 Apoptosis. 2020 Feb;25(1-2):1-11. doi: 10.1007/s10495-019-01575-3.

694 Bastard P, Zhang Q, Zhang SY, Jouanguy E, Casanova JL. Type I interferons and
695 SARS-CoV-2: from cells to organisms. Curr Opin Immunol. 2022 Feb;74:172-182. doi:
696 10.1016/j.coi.2022.01.003.

697 Bojkova D, Klann K, Koch B, Widera M, Krause D, Ciesek S, Cinatl J, Münch C.
698 Proteomics of SARS-CoV-2-infected host cells reveals therapy targets. Nature. 2020
699 Jul;583(7816):469-472. doi: 10.1038/s41586-020-2332-7.

700 Bojkova D, McGreig JE, McLaughlin KM, Masterson SG, Antczak M, Widera M,
701 Krähling V, Ciesek S, Wass MN, Michaelis M, Cinatl J Jr. Differentially conserved
702 amino acid positions may reflect differences in SARS-CoV-2 and SARS-CoV
703 behaviour. Bioinformatics. 2021 Feb 9;37(16):2282-8. doi:
704 10.1093/bioinformatics/btab094.

Bojkova D, Widera M, Ciesek S, Wass MN, Michaelis M, Cinatl J jr. Reduced interferon antagonism but similar drug sensitivity in Omicron variant compared to Delta variant SARS-CoV-2 isolates. Cell Res. 2022 Mar;32(3):319-321.

Bojkova D, Rothenburger T, Ciesek S, Wass MN, Michaelis M, Cinatl J Jr. SARS-CoV-2 Omicron variant virus isolates are highly sensitive to interferon treatment. Cell Discov. 2022a May 10;8(1):42.

Bojkova D, Reus P, Panosch L, Bechtel M, Rothenburger T, Kandler J, Pfeiffer A, Wagner JUG, Shumliakivska M, Dimmeler S, Olmer R, Martin U, Vondran F, Toptan T, Rothweiler F, Zehner R, Rabenau H, Osman KL, Pullan ST, Carroll M, Stack R, Ciesek R, Wass MN, Michaelis M, Cinatl J Jr. Identification of novel antiviral drug candidates using an optimized SARS-CoV-2 phenotypic screening platform. bioRxiv. 2022b Jul 17:2022.07.17.500346. doi: 10.1101/2022.07.17.500346.

Borrelli M, Corcione A, Castellano F, Fiori Nastro F, Santamaria F. Coronavirus Disease 2019 in Children. Front Pediatr. 2021 May 28;9:668484. doi: 10.3389/fped.2021.668484.

Cameroni E, Bowen JE, Rosen LE, Saliba C, Zepeda SK, Culap K, Pinto D, VanBlargan LA, De Marco A, di Iulio J, Zatta F, Kaiser H, Noack J, Farhat N, Czudnochowski N, Havenar-Daughton C, Sprouse KR, Dillen JR, Powell AE, Chen A, Maher C, Yin L, Sun D, Soriaga L, Bassi J, Silacci-Fregni C, Gustafsson C, Franko NM, Logue J, Iqbal NT, Mazzitelli I, Geffner J, Grifantini R, Chu H, Gori A, Riva A, Giannini O, Ceschi A, Ferrari P, Cippà PE, Franzetti-Pellanda A, Garzoni C, Halfmann PJ, Kawaoka Y, Hebner C, Purcell LA, Piccoli L, Pizzuto MS, Walls AC, Diamond MS, Telenti A, Virgin HW, Lanzavecchia A, Snell G, Veesler D, Corti D. Broadly neutralizing antibodies overcome SARS-CoV-2 Omicron antigenic shift. Nature. 2022 Feb;602(7898):664-670. doi: 10.1038/s41586-021-04386-2.

730 Chiale C, Greene TT, Zuniga EI. Interferon induction, evasion, and paradoxical roles
731 during SARS-CoV-2 infection. Immunol Rev. 2022 Jul 1. doi: 10.1111/imr.13113.
732 Cinatl J Jr, Hoever G, Morgenstern B, Preiser W, Vogel JU, Hofmann WK, Bauer G,
733 Michaelis M, Rabenau HF, Doerr HW. Infection of cultured intestinal epithelial cells
734 with severe acute respiratory syndrome coronavirus. Cell Mol Life Sci. 2004
735 Aug;61(16):2100-12. doi: 10.1007/s00018-004-4222-9.
736 Cline TD, Beck D, Bianchini E. Influenza virus replication in macrophages: balancing
737 protection and pathogenesis. J Gen Virol. 2017 Oct;98(10):2401-2412. doi:
738 10.1099/jgv.0.000922.
739 Cuadrado-Payán E, Montagud-Marrahi E, Torres-Elorza M, Bodro M, Blasco M, Poch
740 E, Soriano A, Piñeiro GJ. SARS-CoV-2 and influenza virus co-infection. Lancet. 2020
741 May 16;395(10236):e84. doi: 10.1016/S0140-6736(20)31052-7.
742 Eldesouki RE, Uhteg K, Mostafa HH. The circulation of Non-SARS-CoV-2 respiratory
743 viruses and coinfections with SARS-CoV-2 during the surge of the Omicron variant. J
744 Clin Virol. 2022 Aug;153:105215. doi: 10.1016/j.jcv.2022.105215.
745 Forero A, Ozarkar S, Li H, Lee CH, Hemann EA, Nadjsombati MS, Hendricks MR, So
746 L, Green R, Roy CN, Sarkar SN, von Moltke J, Anderson SK, Gale M Jr, Savan R.
747 Differential Activation of the Transcription Factor IRF1 Underlies the Distinct Immune
748 Responses Elicited by Type I and Type III Interferons. Immunity. 2019 Sep
749 17;51(3):451-464.e6. doi: 10.1016/j.immuni.2019.07.007.
750 Fourati S, Jimenez-Morales D, Hultquist J, Chang MW, Benner C, Krogan N, Pache
751 L, Chanda S, Sekaly R-P, García-Sastre A, Uccellini MB. Type I IFN promotes
752 pathogenic inflammatory monocyte maturation during H5N1 infection. bioRxiv. 2022
753 Jan 11:2022.01.10.475751. doi: 10.1101/2022.01.10.475751.

754 Guo K, Barrett BS, Morrison JH, Mickens KL, Vladar EK, Hasenkrug KJ, Poeschla EM,
755 Santiago ML. Interferon resistance of emerging SARS-CoV-2 variants. Proc Natl Acad
756 Sci U S A. 2022 Aug 9;119(32):e2203760119. doi: 10.1073/pnas.2203760119.
757 Hartshorn KL. Innate Immunity and Influenza A Virus Pathogenesis: Lessons for
758 COVID-19. Front Cell Infect Microbiol. 2020 Oct 22;10:563850. doi:
759 10.3389/fcimb.2020.563850.
760 Hoeve MA, Nash AA, Jackson D, Randall RE, Dransfield I. Influenza virus A infection
761 of human monocyte and macrophage subpopulations reveals increased susceptibility
762 associated with cell differentiation. PLoS One. 2012;7(1):e29443. doi:
763 10.1371/journal.pone.0029443.
764 Hong Q, Han W, Li J, Xu S, Wang Y, Xu C, Li Z, Wang Y, Zhang C, Huang Z, Cong
765 Y. Molecular basis of receptor binding and antibody neutralization of Omicron. Nature.
766 2022 Apr;604(7906):546-552. doi: 10.1038/s41586-022-04581-9.
767 Hu B, Chan JF, Liu H, Liu Y, Chai Y, Shi J, Shuai H, Hou Y, Huang X, Yuen TT, Yoon
768 C, Zhu T, Zhang J, Li W, Zhang AJ, Zhou J, Yuan S, Zhang BZ, Yuen KY, Chu H.
769 Spike mutations contributing to the altered entry preference of SARS-CoV-2 Omicron
770 BA.1 and BA.2. Emerg Microbes Infect. 2022 Aug 30:1-31. doi:
771 10.1080/22221751.2022.2117098.
772 Hui KPY, Ho JCW, Cheung MC, Ng KC, Ching RHH, Lai KL, Kam TT, Gu H, Sit KY,
773 Hsin MKY, Au TWK, Poon LLM, Peiris M, Nicholls JM, Chan MCW. SARS-CoV-2
774 Omicron variant replication in human bronchus and lung ex vivo. Nature. 2022
775 Mar;603(7902):715-720. doi: 10.1038/s41586-022-04479-6.
776 Junqueira C, Crespo Â, Ranjbar S, de Lacerda LB, Lewandrowski M, Ingber J, Parry
777 B, Ravid S, Clark S, Schrimpf MR, Ho F, Beakes C, Margolin J, Russell N, Kays K,
778 Boucau J, Das Adhikari U, Vora SM, Leger V, Gehrke L, Henderson LA, Janssen E,

779 Kwon D, Sander C, Abraham J, Goldberg MB, Wu H, Mehta G, Bell S, Goldfeld AE,
780 Filbin MR, Lieberman J. FcγR-mediated SARS-CoV-2 infection of monocytes
781 activates inflammation. Nature. 2022 Jun;606(7914):576-584. doi: 10.1038/s41586-
782 022-04702-4.
783 Kim EH, Nguyen TQ, Casel MAB, Rollon R, Kim SM, Kim YI, Yu KM, Jang SG, Yang
784 J, Poo H, Jung JU, Choi YK. Coinfection with SARS-CoV-2 and Influenza A Virus
785 Increases Disease Severity and Impairs Neutralizing Antibody and CD4+ T Cell
786 Responses. J Virol. 2022 Mar 23;96(6):e0187321. doi: 10.1128/jvi.01873-21.
787 Kim HK, Kang JA, Lyoo KS, Le TB, Yeo YH, Wong SS, Na W, Song D, Webby RJ,
788 Zanin M, Jeong DG, Yoon SW. Severe acute respiratory syndrome coronavirus 2 and
789 influenza A virus co-infection alters viral tropism and haematological composition in
790 Syrian hamsters. Transbound Emerg Dis. 2022 Jun 1:10.1111/tbed.14601. doi:
791 10.1111/tbed.14601.
792 King C, Sprent J. Dual Nature of Type I Interferons in SARS-CoV-2-Induced
793 Inflammation. Trends Immunol. 2021 Apr;42(4):312-322. doi:
794 10.1016/j.it.2021.02.003.
795 Krumbein H, Kümmel LS, Fragkou PC, Thölken C, Hünerbein BL, Reiter R,
796 Papathanasiou KA, Renz H, Skevaki C. Respiratory viral co-infections in patients with
797 COVID-19 and associated outcomes: A systematic review and meta-analysis. Rev
798 Med Virol. 2022 Jun 10:e2365. doi: 10.1002/rmv.2365.
799 Lamichhane PP, Boonnak K, Changsom D, Noisumdaeng P, Sangsiriwut K,
800 Pattanakitsakul SN, Puthavathana P. H5N1 NS genomic segment distinctly governs
801 the influenza virus infectivity and cytokine induction in monocytic cells. Asian Pac J
802 Allergy Immunol. 2018 Mar;36(1):58-68.

803 Lamichhane PP, Puthavathana P. PR8 virus harbouring H5N1 NS gene contributed
804 for THP-1 cell tropism. Virusdisease. 2018 Dec;29(4):548-552. doi: 10.1007/s13337-
805 018-0499-4.
806 Lee ACY, To KKW, Zhu H, Chu H, Li C, Mak WWN, Zhang AJX, Yuen KY. Avian
807 influenza virus A H7N9 infects multiple mononuclear cell types in peripheral blood and
808 induces dysregulated cytokine responses and apoptosis in infected monocytes. J Gen
809 Virol. 2017 May;98(5):922-934. doi: 10.1099/jgv.0.000751.
810 Lersritwimanmaen P, Na-Ek P, Thanunchai M, Thewsoongnoen J, Sa-Ard-Iam N,
811 Wiboon-ut S, Mahanonda R, Thitithanyanont A. The presence of monocytes enhances
812 the susceptibility of B cells to highly pathogenic avian influenza (HPAI) H5N1 virus
813 possibly through the increased expression of α2,3 SA receptor. Biochem Biophys Res
814 Commun. 2015 Aug 28;464(3):888-93. doi: 10.1016/j.bbrc.2015.07.061.
815 Li N, Parrish M, Chan TK, Yin L, Rai P, Yoshiyuki Y, Abolhassani N, Tan KB, Kiraly O,
816 Chow VT, Engelward BP. Influenza infection induces host DNA damage and dynamic
817 DNA damage responses during tissue regeneration. Cell Mol Life Sci. 2015
818 Aug;72(15):2973-88. doi: 10.1007/s00018-015-1879-1.
819 Li Y, Yu P, Qu C, Li P, Li Y, Ma Z, Wang W, de Man RA, Peppelenbosch MP, Pan Q.
820 MDA5 against enteric viruses through induction of interferon-like response partially via
821 the JAK-STAT cascade. Antiviral Res. 2020 Apr;176:104743. doi:
822 10.1016/j.antiviral.2020.104743.
823 Li L, Han P, Huang B, Xie Y, Li W, Zhang D, Han P, Xu Z, Bai B, Zhou J, Kang X, Li
824 X, Zheng A, Zhang R, Qiao S, Zhao X, Qi J, Wang Q, Liu K, Gao GF. Broader-species
825 receptor binding and structural bases of Omicron SARS-CoV-2 to both mouse and
826 palm-civet ACE2s. Cell Discov. 2022 Jul 12;8(1):65. doi: 10.1038/s41421-022-00431-
827 0.

828 McKellar J, Rebendenne A, Wencker M, Moncorgé O, Goujon C. Mammalian and
829 Avian Host Cell Influenza A Restriction Factors. Viruses. 2021 Mar 22;13(3):522. doi:
830 10.3390/v13030522.
831 McLaughlin KM, Bojkova D, Kandler JD, Bechtel M, Reus P, Le T, Rothweiler F,
832 Wagner JUG, Weigert A, Ciesek S, Wass MN, Michaelis M, Cinatl J Jr. A Potential
833 Role of the CD47/SIRPalpha Axis in COVID-19 Pathogenesis. Curr Issues Mol Biol.
834 2021 Sep 22;43(3):1212-1225. doi: 10.3390/cimb43030086.
835 Meng B, Abdullahi A, Ferreira IATM, Goonawardane N, Saito A, Kimura I, Yamasoba
836 D, Gerber PP, Fatihi S, Rathore S, Zepeda SK, Papa G, Kemp SA, Ikeda T, Toyoda
837 M, Tan TS, Kuramochi J, Mitsunaga S, Ueno T, Shirakawa K, Takaori-Kondo A,
838 Brevini T, Mallery DL, Charles OJ; CITIID-NIHR BioResource COVID-19
839 Collaboration; Genotype to Phenotype Japan (G2P-Japan) Consortium; Ecuador-
840 COVID19 Consortium, Bowen JE, Joshi A, Walls AC, Jackson L, Martin D, Smith KGC,
841 Bradley J, Briggs JAG, Choi J, Madissoon E, Meyer KB, Mlcochova P, Ceron-
842 Gutierrez L, Doffinger R, Teichmann SA, Fisher AJ, Pizzuto MS, de Marco A, Corti D,
843 Hosmillo M, Lee JH, James LC, Thukral L, Veesler D, Sigal A, Sampaziotis F,
844 Goodfellow IG, Matheson NJ, Sato K, Gupta RK. Altered TMPRSS2 usage by SARS-
845 CoV-2 Omicron impacts infectivity and fusogenicity. Nature. 2022 Mar;603(7902):706-
846 714. doi: 10.1038/s41586-022-04474-x.
847 Oishi K, Horiuchi S, Minkoff JM, tenOever BR. The Host Response to Influenza A Virus
848 Interferes with SARS-CoV-2 Replication during Coinfection. J Virol. 2022 Aug
849 10;96(15):e0076522. doi: 10.1128/jvi.00765-22.
850 Peacock TP, Goldhill DH, Zhou J, Baillon L, Frise R, Swann OC, Kugathasan R, Penn
851 R, Brown JC, Sanchez-David RY, Braga L, Williamson MK, Hassard JA, Staller E,
852 Hanley B, Osborn M, Giacca M, Davidson AD, Matthews DA, Barclay WS. The furin

853 cleavage site in the SARS-CoV-2 spike protein is required for transmission in ferrets.
854 Nat Microbiol. 2021 Jul;6(7):899-909. doi: 10.1038/s41564-021-00908-w.
855 Prokunina-Olsson L, Alphonse N, Dickenson RE, Durbin JE, Glenn JS, Hartmann R,
856 Kotenko SV, Lazear HM, O'Brien TR, Odendall C, Onabajo OO, Piontkivska H, Santer
857 DM, Reich NC, Wack A, Zanoni I. COVID-19 and emerging viral infections: The case
858 for interferon lambda. J Exp Med. 2020 May 4;217(5):e20200653. doi:
859 10.1084/jem.20200653.
860 Rani MR, Croze E, Wei T, Shrock J, Josyula A, Kalvakolanu DV, Ransohoff RM.
861 STAT-phosphorylation-independent induction of interferon regulatory factor-9 by
862 interferon-beta. J Interferon Cytokine Res. 2010 Mar;30(3):163-70. doi:
863 10.1089/jir.2009.0032.
864 Rathnasinghe R, Jangra S, Ye C, Cupic A, Singh G, Martínez-Romero C, Mulder LCF,
865 Kehrer T, Yildiz S, Choi A, Yeung ST, Mena I, Gillespie V, De Vrieze J, Aslam S,
866 Stadlbauer D, Meekins DA, McDowell CD, Balaraman V, Corley MJ, Richt JA, De
867 Geest BG, Miorin L; PVI study group, Krammer F, Martinez-Sobrido L, Simon V,
868 García-Sastre A, Schotsaert M. Characterization of SARS-CoV-2 Spike mutations
869 important for infection of mice and escape from human immune sera. Nat Commun.
870 2022 Jul 7;13(1):3921. doi: 10.1038/s41467-022-30763-0.
871 Shrestha LB, Foster C, Rawlinson W, Tedla N, Bull RA. Evolution of the SARS-CoV-
872 2 omicron variants BA.1 to BA.5: Implications for immune escape and transmission.
873 Rev Med Virol. 2022 Jul 20:e2381. doi: 10.1002/rmv.2381.
874 Shuai H, Chan JF, Hu B, Chai Y, Yuen TT, Yin F, Huang X, Yoon C, Hu JC, Liu H, Shi
875 J, Liu Y, Zhu T, Zhang J, Hou Y, Wang Y, Lu L, Cai JP, Zhang AJ, Zhou J, Yuan S,
876 Brindley MA, Zhang BZ, Huang JD, To KK, Yuen KY, Chu H. Attenuated replication

877 and pathogenicity of SARS-CoV-2 B.1.1.529 Omicron. Nature. 2022
878 Mar;603(7902):693-699. doi: 10.1038/s41586-022-04442-5.
879 Stowe J, Tessier E, Zhao H, Guy R, Muller-Pebody B, Zambon M, Andrews N, Ramsay
880 M, Lopez Bernal J. Interactions between SARS-CoV-2 and influenza, and the impact
881 of coinfection on disease severity: a test-negative design. Int J Epidemiol. 2021 Aug
882 30;50(4):1124-1133. doi: 10.1093/ije/dyab081.
883 Swets MC, Russell CD, Harrison EM, Docherty AB, Lone N, Girvan M, Hardwick HE;
884 ISARIC4C Investigators, Visser LG, Openshaw PJM, Groeneveld GH, Semple MG,
885 Baillie JK. SARS-CoV-2 co-infection with influenza viruses, respiratory syncytial virus,
886 or adenoviruses. Lancet. 2022 Apr 16;399(10334):1463-1464. doi: 10.1016/S0140-
887 6736(22)00383-X.
888 Thorne LG, Bouhaddou M, Reuschl AK, Zuliani-Alvarez L, Polacco B, Pelin A, Batra
889 J, Whelan MVX, Hosmillo M, Fossati A, Ragazzini R, Jungreis I, Ummadi M, Rojc A,
890 Turner J, Bischof ML, Obernier K, Braberg H, Soucheray M, Richards A, Chen KH,
891 Harjai B, Memon D, Hiatt J, Rosales R, McGovern BL, Jahun A, Fabius JM, White K,
892 Goodfellow IG, Takeuchi Y, Bonfanti P, Shokat K, Jura N, Verba K, Noursadeghi M,
893 Beltrao P, Kellis M, Swaney DL, García-Sastre A, Jolly C, Towers GJ, Krogan NJ.
894 Evolution of enhanced innate immune evasion by SARS-CoV-2. Nature. 2022
895 Feb;602(7897):487-495. doi: 10.1038/s41586-021-04352-y.
896 van Wetering S, van der Linden AC, van Sterkenburg MA, de Boer WI, Kuijpers AL,
897 Schalkwijk J, Hiemstra PS. Regulation of SLPI and elafin release from bronchial
898 epithelial cells by neutrophil defensins. Am J Physiol Lung Cell Mol Physiol. 2000
899 Jan;278(1):L51-8. doi: 10.1152/ajplung.2000.278.1.L51.
900 Wang C, Liu B, Zhang S, Huang N, Zhao T, Lu QB, Cui F. Differences in incidence
901 and fatality of COVID-19 by SARS-CoV-2 Omicron variant versus Delta variant in

relation to vaccine coverage: a world-wide review. J Med Virol. 2022 Sep 2. doi: 10.1002/jmv.28118.

Westenius V, Mäkelä SM, Julkunen I, Österlund P. Highly Pathogenic H5N1 Influenza A Virus Spreads Efficiently in Human Primary Monocyte-Derived Macrophages and Dendritic Cells. Front Immunol. 2018 Jul 17;9:1664. doi: 10.3389/fimmu.2018.01664.

Xiang X, Wang ZH, Ye LL, He XL, Wei XS, Ma YL, Li H, Chen L, Wang XR, Zhou Q. Co-infection of SARS-COV-2 and Influenza A Virus: A Case Series and Fast Review. Curr Med Sci. 2021 Feb;41(1):51-57. doi: 10.1007/s11596-021-2317-2.

Yin X, Riva L, Pu Y, Martin-Sancho L, Kanamune J, Yamamoto Y, Sakai K, Gotoh S, Miorin L, De Jesus PD, Yang CC, Herbert KM, Yoh S, Hultquist JF, García-Sastre A, Chanda SK. MDA5 Governs the Innate Immune Response to SARS-CoV-2 in Lung Epithelial Cells. Cell Rep. 2021 Jan 12;34(2):108628. doi: 10.1016/j.celrep.2020.108628.

Yu WC, Chan RW, Wang J, Travanty EA, Nicholls JM, Peiris JS, Mason RJ, Chan MC. Viral replication and innate host responses in primary human alveolar epithelial cells and alveolar macrophages infected with influenza H5N1 and H1N1 viruses. J Virol. 2011 Jul;85(14):6844-55. doi: 10.1128/JVI.02200-10.

Yue H, Zhang M, Xing L, Wang K, Rao X, Liu H, Tian J, Zhou P, Deng Y, Shang J. The epidemiology and clinical characteristics of co-infection of SARS-CoV-2 and influenza viruses in patients during COVID-19 outbreak. J Med Virol. 2020 Nov;92(11):2870-2873. doi: 10.1002/jmv.26163.

Zhang J, Cai Y, Lavine CL, Peng H, Zhu H, Anand K, Tong P, Gautam A, Mayer ML, Rits-Volloch S, Wang S, Sliz P, Wesemann DR, Yang W, Seaman MS, Lu J, Xiao T, Chen B. Structural and functional impact by SARS-CoV-2 Omicron spike mutations. Cell Rep. 2022 Apr 26;39(4):110729. doi: 10.1016/j.celrep.2022.110729.